A comparative study of Raman enhancement in capillaries

Fatemeh Eftekhari,[a] Juan Irizar, Laila Hulbert, and Amr S. Helmy
Department of Electrical and Computer Engineering, University of Toronto, Toronto, Ontario M5S 3G4, Canada

(Received 16 March 2011; accepted 18 April 2011; published online 6 June 2011)

This work reports on the comparative studies of Raman enhancement in liquid core waveguides (LCWs). The theoretical considerations that describe Raman enhancement in LCWs is adapted to analyze and compare the performance of hollow core photonic crystal fibers (HCPCFs) to conventional Teflon capillary tubes. The optical losses in both platforms are measured and used to predict their performance for different lengths. The results show that for an optimal waveguide length, two orders of magnitude enhancement in the Raman signal can be achieved for aqueous solutions using HCPCFs. This length, however, cannot be achieved using normal capillary effects. By integrating the interface of the fluidic pump and the HCPCF into a microfluidic chip, we are able to control fluid transport and fill longer lengths of HCPCFs regardless of the viscosity of the sample. The long-term stability and reproducibility of Raman spectra attained through this platform are demonstrated for naphthalenethiol, which is a well-studied organic compound. Using the HCPCF platform, the detection limit of normal Raman scattering in the range of micro-molars has been achieved. In addition to the higher signal-to-noise ratio of the Raman signal from the HCPCF-platform, more Raman modes of naphthalenethiol are revealed using this platform. © *2011 American Institute of Physics*. [doi:10.1063/1.3592961]

I. INTRODUCTION

Raman spectroscopy offers great intrinsic specificity, which is well-suited to detect changes that occur at the molecular level. However, studying biological specimens using Raman spectroscopy is associated with unique challenges. Most often, Raman spectroscopy lacks the signal strength required by many biomedical applications for fast real-time measurements.[1] The main challenge at present is the high laser intensity required to retrieve a Raman spectrum with a useful signal-to-noise ratio from dilute and small sample volumes. The negative optical and thermal effects of high-intensity laser excitation on photosensitive biological specimens are limiting the widespread application of Raman spectroscopy techniques in biosensing and analysis.

The emergence of hollow core fibers generates new opportunities for spectroscopic applications, especially since guided modes within the fiber can confine light into small areas, leading to high intensities over long distances.[2,3] The ability to inject a solution into the central air core of these fibers offers huge advantages for strong analyte-light interaction due to the confinement of both the excitation light and the liquid sample in the core. The active sensing area is significantly increased and as a result, Raman spectroscopy in the liquid-core waveguide platform has demonstrated a substantial enhancement in Raman signal.[4,5] With regard to sensing applications, the efficiency of the LCW Raman platform depends on the interaction length between the light and the liquid sample along with the confinement of the excitation laser to the liquid core.

There have been several reports on the utilization of LCWs as biological and chemical sensors.[4–6,9,12] The two most common forms of LCWs that have been investigated to date are Teflon AF-2400 capillary tubing and photonic crystal fibers. Teflon AF-coated capillary tubing has long been the only fiber that can guide light while being filled with low index materials common in aqueous solutions.[13,14] A wide range of wavelengths can be confined and guided in a teflon capillary tube (TCT) core using total internal reflection (TIR).

Alternatively, HCPCFs can guide light in an air core by using the photonic bandgap guidance mechanism. In HCPCFs the air core is formed by a larger central hole surrounded by a 2-D lattice of smaller holes of the cladding. These holes can be filled with a liquid or gas of interest and since the air-filling fraction of the cladding is high, the average index of the cladding is lower than that of the liquid core. The bandwidth of the HCPCF is determined by the cladding hole arrangement and the refractive index of the material filling the holes.[7,8] A highly attractive aspect of this configuration is that the mode field is almost completely confined to the liquid sample and the high light-matter interaction cross-section leads to a significant enhancement in the detection sensitivity while requiring a very small volume of the sample.[10,15–17] By selectively filling the core of the HCPCF while the cladding holes are kept sealed with air, substantial enhancement of Raman signals were obtained from dilute Zn and CdTe nanoparticles in solution which makes the HCPCF a good candidate for *in situ* monitoring of colloidal nanoparticle synthesis and DNA molecular interactions.[23–25]

However, in all the HCPCF-based sensing templates reported to date, fluid infiltrated the channels either by capillary effect, where the short liquid filling length restricts the potential detection efficiency, or by using a pressure cell,

[a]Author to whom correspondence should be addressed. Electronic mail: z.eftekhari@gmail.com.

which requires large-scale specialized laboratory equipment. This excessive pressure results in a damaged cladding in the photonic crystal fiber.[7,11] In addition, passive capillary filling each strand of HCPCF is only usable one time and proper draining and flushing of contaminants is not attainable using capillary action.

In this paper, by implementing the interface of the fluidic pump and the HCPCF onto a microfluidic chip, an approach to utilize, and hence harvest, a useful Raman signal from a long fiber length is demonstrated. This opens up the possibility of using the LCWs strands for multi-stage experiments. This technique shows further enhancement of the detection sensitivity using Raman spectroscopy due to the enhanced light-analyte overlap over a long interaction length. The theory that has been developed for Raman enhancements in conventional LCWs is adapted to encompass HCPCFs operating in a TIR regime. The calculations are carried out to characterize both the TCTs and HCPCFs enhancement for Raman spectroscopy. The developed platforms are highly suited for biological sensing applications, where low-power laser irradiation is needed to maintain the sample integrity. This scheme also takes advantage of low transmission loss, which enables the use of longer fiber lengths and hence enables the maximization of the Raman signal.

II. EXAMINING THE RAMAN ENHANCEMENT FROM TCT AND HCPCF

The enhancement technique in all LCW platforms is mostly based on its use as a waveguide to confine both the liquid and the optical field over a long distance to obtain a larger light-matter interaction length. As a result, Raman scattering can be efficiently excited along the fiber's entire length, and Raman modes are also guided by the fiber and can be collected through the same waveguide. In this section, the performance of TCT- and HCPCF-platforms for Raman spectroscopy are analyzed and compared.

The TCTs with average core diameters of $d_{\mathrm{TCT}} = 115$ μm were obtained from Biogeneral. Two types of HCPCFs (HC800 andHC1060), were purchased from Crystal Fiber. Their physical and optical properties are summarized in Table I. In all of the modeling and experiments carried out in this work, the sample solution is selectively injected only into the hollow core of the HCPCF, leaving the cladding voids filled with air.

The degree of Raman enhancement attained for a specific solution using TCT- or HCPCF- platforms depends on the physical parameters of the waveguide. In a given LCW platform, the intensity of the Raman signal, which is obtained in a backscattering configuration is of the form,

$$I_{\mathrm{LCW}} = \frac{P_o}{2\alpha}\rho\sigma\pi NA\left(1 - e^{-2\alpha L}\right), \tag{1}$$

where P_o is the fraction of laser power coupled into the waveguide, α is the loss coefficient of the waveguide, NA is the numerical aperture of the waveguide, and L is the length of fiber filled with solution. The characteristics of the sample solution itself, referring to the Raman cross-section and the number of scattering centers per unit volume of the sample solution are ρ and σ, respectively[2]. Physical insight into the Raman enhancement in the LCWs used in this work can be achieved by investigating the waveguiding properties of both systems in more detail.

Since both the pump laser and the Raman scattered signal are propagating along the same waveguide, the efficiency of direct coupling of a laser source into the LCW and the detection efficiency of the collected Raman signal depend on the numerical aperture of the fiber. The coupling efficiency of the laser pump depends on the acceptance angle of the radiation, which is limited by the critical angle of the mode that is guided by TIR. On the contrary, only the fraction of Raman scattering that falls within the critical angle of the waveguide will be coupled into guided modes in the core and can be collected through propagation in the TIR mode up to the edge of the LCW. The NA can be described in terms of the refractive index contrast between the core and cladding,

$$NA = \sqrt{\left(n_{eff}^{core}\right)^2 - \left(n_{eff}^{clad}\right)^2}. \tag{2}$$

For TCT the refractive index of the Teflon cladding is 1.29, but for the HCPCFs, due to the complex periodic voids in the cladding, defining n_{eff}^{clad} is not straightforward and several methods have been developed for its computation, including a fully analytical vectorial approach.[26] In this method, the n_{eff}^{clad} of a HCPCF can be determined by calculating the corresponding effective index.

Using the definition of the air-filling fraction for a triangular structure, $(\pi/2\sqrt{3})(d_{clad}/\Lambda)^2$, the d_{clad} for both HC800 and HC1060 are obtained. Two different numerical approaches, the beam propagation method using BeamProp Rsoft, and the finite-difference time-domain using FDTD Mode Solver, along with an open source Python script based on the set of analytical mode solutions of HCPCFs developed by Midrio *et al.*[26] are implemented to compute the value of n_{eff}^{clad} of both fibers at the HeNe excitation wavelength, $\lambda = 632$ nm. The results from both numerical and analytical methods showed very good agreement and n_{eff}^{clad} are computed as 1.14 for HC800 and 1.17 for HC1060. Figure 1 shows the calculated Raman intensity normalized to the intensity with $NA = 1$, for TCTs and HCPCFs (HC800) by varying the refractive index of the core. As can clearly be seen, although the NA depends on the sample solution used in both TCTs and HCPCFs, NA is considerably larger for the HCPCF ($\approx$0.68 for water) than for the TCT ($\approx$0.32 for

TABLE I. Physical and optical parameters for air-guiding HCPCFs, which are used in this work.

Parameters	HC800	HC1060
Core diameter	10 μm	9.5 μm
Pitch	2.3 μm	2.75 μm
Center operating wavelength	830 nm	1060 nm
Transmission bands	>70 nm	>90 nm
Air-filling fraction	>90%	>90%

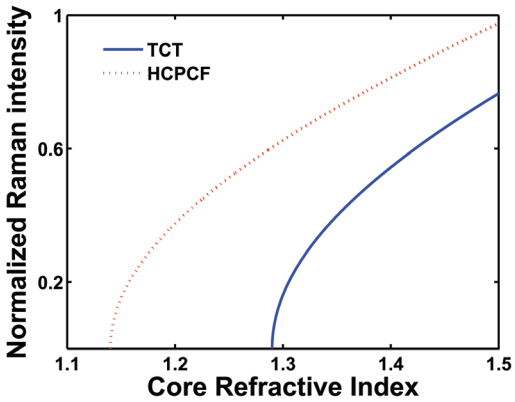

FIG. 1. (Color online) Calculated normalized Raman intensity attained from the HCPCF (HC800) and the TCT with varying refractive index of the core.

water) due to the higher index contrast between the core and cladding. The difference between the *NA* of the TCT and the HCPCF becomes smaller for higher refractive index solutions.

Further insights of Raman enhancements in the waveguides used in this work were obtained by studying the effect of the LCW length on the Raman intensity of a specific mode. The analysis was carried out by measuring the Raman intensity of the water mode centered at around 3400 cm^{-1} for varying practical usable lengths of TCTs and HC800. A plot of the intensity of this mode as a function of waveguide length is shown in Fig. 2. The collected experimental data is fitted to Eq. (1) using two parameters: α and a new defined parameter, $\kappa = P_o \rho \pi NA$. The attenuation length, α^{-1}, was found to be 144 cm for the TCT and 267 cm for the HCPCF. A previous report by Altkorn *et al.* investigated the optical losses in TCTs featuring similar dimensions and excitation conditions to those used in this work.[2] They reported an absorption length of $\alpha^{-1} = 150$ cm which agrees very well with the results obtained in this work.

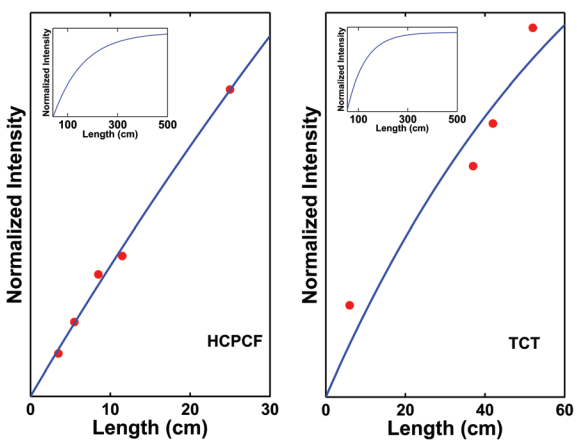

FIG. 2. (Color online) Fitting of experimental data to Eq. (1) for (left) HC800 and (right) TCT. The intensities are normalized with respect to the intensity obtained with a cuvette. Insets: Predictable plateau of intensity for the LCW over the practical length scale. The first cladding mode in the infinite periodic structure often denoted as the fundamental space filling mode. By definition, this mode exhibits the highest effective index, zero transverse wavevector, and it fills all of the space. The value of n_{eff}^{clad} is a function of the wavelength, λ, the dielectric constant of silica, ε_{silica}, the air-hole pitch, and the cladding air-hole diameter d_{clad} (Ref. 26).

There is no data available to compare the computed absorption length for HCPCFs, and to the best of our knowledge, this is the first report of a measurement in a HCPCF with a liquid-filled core. By comparing the absorption length of a TCT and a HCPCF, for the waveguide- length range used in this report, guiding in TCTs would impose higher losses on the collected Raman signal.

From the fitting parameters, the value of maximum Raman enhancements attainable through TCTs and HCPCFs were also computed from $P_{max} = \kappa/2\alpha$. The calculation results show that for an optimal waveguide length, two orders of magnitude more enhancement can be achieved for aqueous solutions using HCPCFs. This length, however, cannot be achieved using normal capillary effects. The platform reported here enables us to control fluid transport and fill-longer lengths of HCPCFs regardless of the viscosity of the sample.

III. EXPERIMENTAL SETUP

Microfluidics offers a set of exciting properties, which makes them suitable platforms for miniaturized biological studies. Two poly(dimethylsiloxane) (PDMS) microfluidic chips were developed to control the fluid delivery into the hollow core and collect the sample from the other side. PDMS is compatible with most biological and chemical materials while it is inexpensive, flexible, and optically transparent down to 230 nm. In addition, the techniques for fabricating PDMS microstructures are well-established and if desired, many PDMS replicas can be made from a single master. Both of the chips were irreversibly sealed to individual glass cover slips by oxygen plasma treatment, and can withstand pressures of 30–50 psi.[18]

In order to selectively fill the central core of the HCPCF with solution, a fusion splicing technique was used to selectively seal the cladding voids at both end facets.[19] High temperatures during the fusion process cause the small capillaries to collapse into each other, while the central core remains largely unaffected due to its larger diameter. By adjusting the fusion current, fusion duration, and position of the HCPCF, the cladding voids can be precisely sealed. This is especially important for the fiber-end that is used for laser coupling.

The ends of the LCW fibers (30 cm long TCT and 15 cm long HCPCF) were inserted into flow chambers in the two separate microfluidic chips. The sample solution was first introduced into the chip and afterward into the LCW using a syringe pump. The volume of the sample needed to fill the chip is about 4 μl.

The schematic diagram of the experimental setup is shown in Fig. 3. Microscope objective lenses (10 × and 50 ×) were used to couple the exciting 632 nm HeNe laser into the TCT and HCPCF, respectively. Both objectives were chosen with respect to their numerical apertures, to provide maximum coupling efficiency. The backscattered Raman signal was collected though the same objective lens into the Raman spectrometer (JY Horriba HR800 LabRam). To ensure that the collected spectrum was from the core and not the fiber cladding, the Raman spectrum of the air-filled

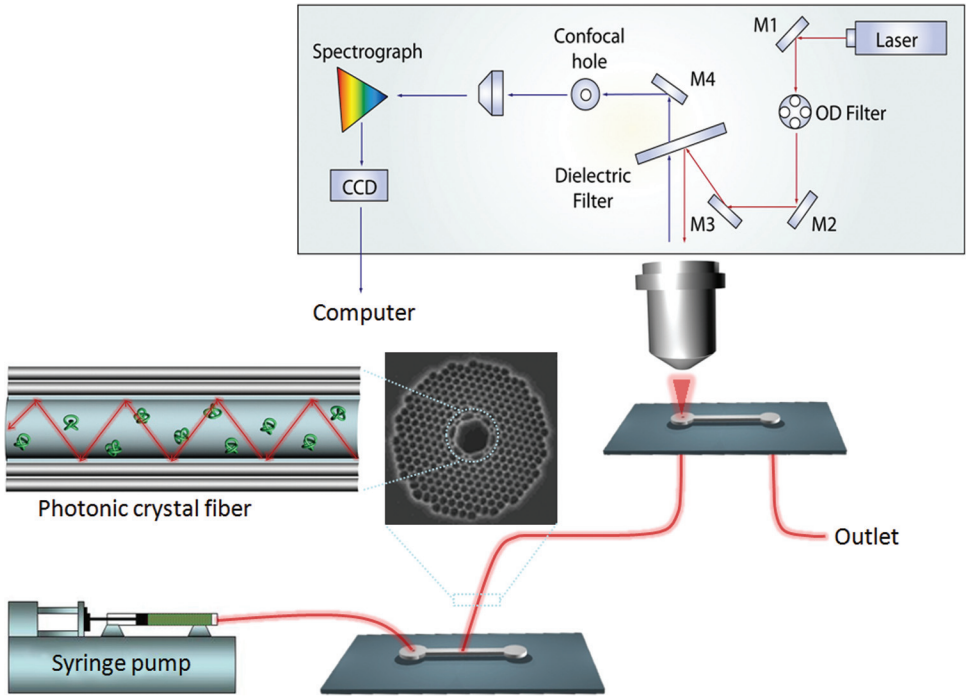

FIG. 3. (Color online) Schematic diagram of the experimental setup. The solution of interest is injected into the central core of the LCW and excited by a HeNe laser.

fiber was investigated and showed minimal spectral interference from silica.

IV. EXPERIMENTAL RESULTS

In order to illustrate the capability of LCWs as a Raman platform to monitor the concentration of a specific analyte solution, different molar ratios of 1-naphthalenethiol (NPT) to methanol were injected into the central core of TCTs and HCPCFs (HC800). The long-term stability of our experimental setup has been measured and verified for various time intervals up to 1 h. The concentration dependency of the intensity of the Raman lines was studied using the TCT-platform. The collected Raman spectra are shown in Fig. 4(top). While methanol Raman bands are also present, the additional Raman peaks between 300 and 3000 cm^{-1} are characteristic of various vibrational modes in NPT, which match well with the previous theoretically calculated Raman bands.[20]

In the two bottom figures of Fig. 4, the intensity of the NPT characteristic Raman lines changes in proportion to the concentration of the sample. The linear correlation between the Raman intensity and the NPT concentration shows how this technique can be used for real-time monitoring of the analyte concentration in a solution of interest. The lowest NPT concentration with detectable Raman modes was found to be 500 μM using the TCT-platform. A similar experiment was then carried out with HC800 and a much larger enhancement of the Raman signal was observed. In addition, the limit of detection was found to be 10 μM with the HCPCF-platform. This significant improvement in sensitivity is due to the small size of the HCPCF's core which leads to higher optical intensity confinement in the central core. A higher fraction of the laser electric field interacts with the sample solution, increasing the detection sensitivity.

Figure 5 shows a comparison between the Raman spectra of methanol acquired with the TCT- and HCPCF-platforms. In addition to the dramatic increase in the intensity of the methanol Raman bands with a higher signal-to-noise ratio, more Raman modes are revealed through using the HCPCF. We also found that significantly shorter scanning periods are needed with the HCPCF-platform to detect an even lower amount of the molecular concentration.

The performance of the HCPCF platform in Raman enhancement was further experimentally assessed by comparing the intensity of the Raman spectra acquired using two different HCPCFs with central operating wavelengths of 800 nm (HC800) and 1060 nm (HC1060). The equal-length strands of both HCPCFs were loaded with methanol and Raman spectra were obtained under the same conditions of laser excitation intensity and acquisition time. Compared to HC800, an increase of 30% in Raman intensity was observed with HC1060 for methanol bands around 1049, 1467, 2848, and 2956 cm^{-1}. Since the *NA* of both fibers are the same, this enhancement may be understood by considering light confinement and guidance mechanism in HCPCFs.

The principle of light confinement and guidance in HCPCFs has been investigated both experimentally and theoretically by several groups.[15,16,22] It has been shown that for $n_c > n_{eff}^{clad}$, light is confined and propagates in the core and it is evanescent in the cladding region. Although the confinement is mainly through TIR, some waveguiding can also be ascribed to bandgap effects.

Upon filling the HCPCF by the sample solution, the guided wavelength range shifts to a new wavelength, and the shifted wavelength is given by,

$$\lambda = \lambda_0 \left(\frac{n_s^2 - n_h^2}{n_s^2 - 1} \right)^{1/2}, \quad (3)$$

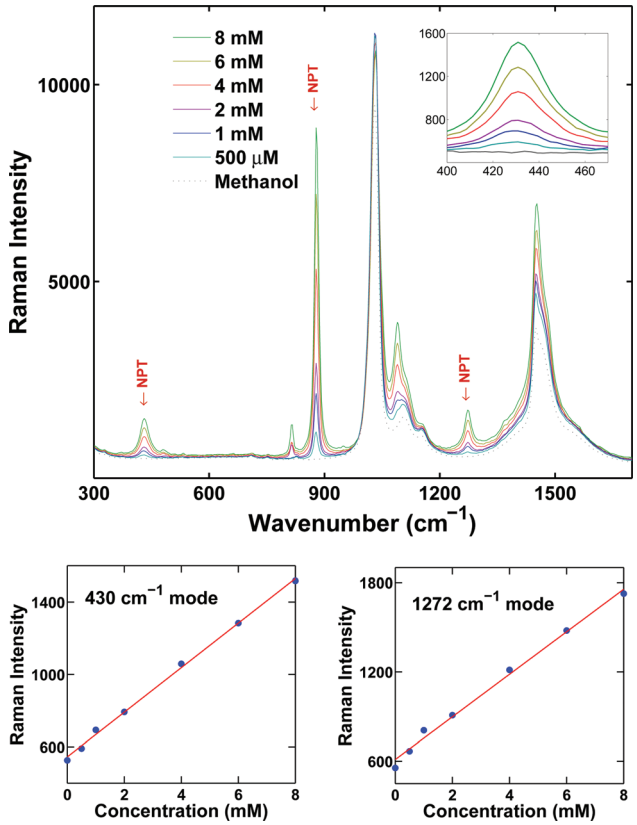

FIG. 4. (Color online) (Top) Normal Raman spectra acquired using a TCT filled with different concentrations of NPT and methanol as a buffer. Concentration dependence curve for NPT Raman-active modes at (left-bottom) 430 cm^{-1}, and (right-bottom) 1272 cm^{-1}.

where n_s is the refractive index of the solid material, and n_h is the refractive index of the liquid.[21] Thus, the guiding wavelength regime of HC1060 coincides with the HeNe laser wavelength when it is filled with either methanol- or water-based solutions. Another reason behind the signal enhancement might also be due to the 5% smaller core radius of HC1060 that could lead to a higher optical intensity confined in the core.

One practical consideration is the potential for reusing the HCPCF and TCT platforms for multiple measurements during a multi-stage experiment. The filling and cleaning procedures of the HCPCF core can be achieved with an alternative use of a miniature diaphragm vacuum pump (Hargraves) and a syringe pump, and we could successfully clean both TCTs and HCPCFs with methanol and isopropanol alcohol.

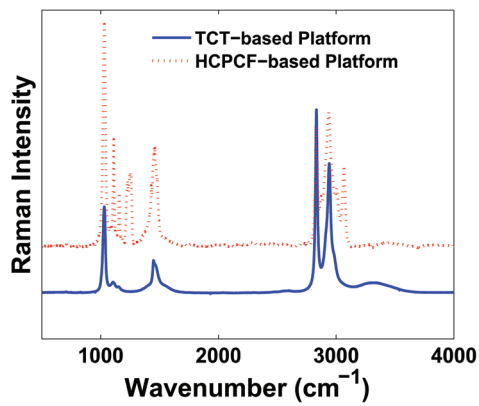

FIG. 5. (Color online) Comparison between the Raman spectra of methanol acquired using the TCT-based platform and the HCPCF-based platform.

V. CONCLUSION

In conclusion, we have demonstrated the significant potential of the HCPCF as a robust sensing and analytical platform for spontaneous Raman scattering of ultratrace analytes in solution with minimal spectral interference from the fiber constituent silica. Confinement of the excitation laser and analyte inside the core of a LCW, and consequently strong light-analyte overlap over the entire length of the LCW yields significant Raman intensity enhancements. The optical losses in both fibers have been measured by studying the effect of the LCW length on the Raman intensity of a specific water mode. The theoretical comparison of Raman enhancements in both LCWs has shown that for an optimal LCW's length, two orders of magnitude more enhancement can be achieved using HCPCF for aqueous samples. However, capillary forces cannot draw a column of liquid to any arbitrary length. The developed platform enables us to fill longer lengths of HCPCFs regardless of the viscosity of the sample solution. The Raman spectra attained through this platform have exhibited good reproducibility and long-term stability. Specifically, using the HCPCF platform, the detection limit of normal Raman scattering in the range of micromolar has been achieved. In addition to a higher signal-to-noise ratio of the Raman signal from the HCPCF-platform, more Raman modes are revealed using this platform. The linear dependence of the Raman signal to the concentration of the solution renders the reported platform practical for various analytical and sensing applications. In addition to improving the sensitivity of normal Raman spectroscopy, a capillary waveguide can provide flexibility, convenient sampling, and remote sensing capability. In our future work, we consider examining the capability of the LCW Raman platform to study biomolecular interactions, such as protein-ligand binding.

[1]K. Kneipp, H. Kneipp, and I. Itzkan, Chem. Rev. **99**, 2957 (1999).
[2]R. Altkorn, M. D. Malinsky, R. P. Van Duyne, and I. Koev, Appl. Spectrosc. **55**, 373 (2001).
[3]S. Smolka, M. Barth, and O. Benson, Opt. Express **15**, 12783 (2007).
[4]M. Holtz, P. K. Dasgupta, and G. Zhang, Anal. Chem. **71**, 2934 (1999).
[5]X. Yang, C. Shi, D. Wheeler, R. Newhouse, B. Chen, J. Z. Zhang, and C. Gu, J. Opt. Soc. Am. A **27**, 977 (2010).
[6]F. Benabid, F. Couny, J. C. Knight, T. A. Birks, and P. St. J. Russell, Nature (London) **434**, 488 (2005).
[7]F. Benabid, J. C. Knight, G. Antonopoulos, and P. St. J. Russell, Science **298**, 5592 399 (2002).
[8]A. Argyros and J. Pla, Opt. Express **15**, 7713 (2007).
[9]S. O. Konorov, C. J. Addison, H. G. Schulze, R. F. B. Turner, and M. W. Blades, Opt. Lett. **31**, 1911 (2006).
[10]F. M. Cox, A. Argyros, and M. C. J. Large, Opt. Express **14**, 4135 (2006).
[11]F. M. Cox, A. Argyros, M. C. J. Large, and S. Kalluri, Opt. Express **15**, 13675 (2007).
[12]H. Yan, C. Gu, C. Yang, J. Liu, G. Jin, J. Zhang, L. Hou, and Y. Yao, Appl. Phys. Lett. **89**, 204101 (2006).
[13]R. Altkorn, I. Koev, and M. J. Pelletier, Appl. Spectrosc. **53**, 1169 (1999).
[14]M. J. Pelletier and R. Altkorn, Anal. Chem. **73**(6), 1393 (2001).

[15]Y. Zhang, C. Shi, C. Gu, L. Seballos, and J. Z. Zhang, Appl. Phys. Lett. **90**, 193504 (2007).
[16]J. Sun, C. C. Chan, Y. F. Zhang, and P. Shum, J. Biomed. Opt. **13**, 054048 (2008).
[17]S. Smolka, M. Barth, and O. Benson, Appl. Phys. Lett. **90**, 111101 (2007).
[18]S. K. Sia and G. M. Whitesides, Electrophoresis **24**, 3563 (2003).
[19]L. Xiao, W. Jin, M. Demokan, H. Ho, Y. Hoo, and Ch. Zhao, Opt. Express **13**, 9014 (2005)
[20]R. A. Alvarez-Puebla, D. S. Dos Santos Jr., and R. F. Aroca, Analyst **129**, 1251 (2004).
[21]G. Antonopoulos, F. Benabid, T. A. Birks, D. M. Bird, J. C. Knight, and P. St. J. Russell, Opt. Express **14**, 3000 (2006).
[22]R. F. Cregan, B. J. Mangan, J. C. Knight, T. A. Birks, P. St. J. Russell, P. J. Roberts, and D. C. Allan, Science **285**, 1537 (1999).
[23]J. Irizar, J. Dinglasan, J. B. Goh, A. Khetani, H. Anis, D. Anderson, C. Goh, and A. S. Helmy, IEEE J Select Top Quantum Electron. **14**, 1214 (2008).
[24]S. A. Rutledge, A. A. Farah, J. Dinglasan, D. J. Anderson, A. Das, J. Goh, C. Goh, and A. S. Helmy, ACS J. Phys. Chem. C **113**, 20208 (2009).
[25]R. M. Abu-Ghazalah, J. Irizar, A. S. Helmy, and R. B. Macgregor, Jr., Biophys. Chem. **147**, 3 123 (2009).
[26]M. Midrio, M. P. Singh, and C. G. Someda, J. Lightwave Technol. **18**, 1031 (2000).